Nonconnected atomic surfaces for quasicrystalline sphere packings

Eric Cockayne*
Laboratory of Atomic and Solid State Physics, Cornell University, Ithaca, New York 14853
(Received 23 August 1993)

The problem of maximizing the density of quasiperiodic sphere packings is investigated. The investigation is limited primarily to the case where the centers of the spheres are determined by a cut through a higher-dimensional Bravais lattice of a single atomic surface. For certain cases, the sphere packing obtained by the largest connected atomic surface can be made more dense by replacing it with an atomic surface that is nonconnected. The nonconnected atomic surfaces differ from the connected ones only in specific regions near the atomic surface boundaries. These regions are determined by the quasicrystalline point-group symmetry and by the radius of the spheres. This method of improving sphere packings is applied to find nonconnected atomic surfaces for the dodecagonal, octagonal, and icosahedral cases. Using this method in conjunction with other methods, a packing fraction of approximately 0.5645 for a simple icosahedral *b*-*c* network is achieved.

I. INTRODUCTION

The problem of finding dense quasiperiodic sphere packings is of interest in the field of quasicrystals for several reasons. To find a plausible atomic structure for a quasicrystal, a "packing" of atoms must be found, subject to information about near-neighbor distances, that agrees with the experimental density.[1-3] In addition, in cluster-based models of quasicrystals,[4-6] where a high density of clusters is desired, the clusters themselves are similar to spheres in a sphere packing. Furthermore, studies of the stability of quasicrystalline structures using pair potentials appear to favor structures corresponding to high-density sphere packings.[7]

Various methods are known for generating quasiperiodic structures. These include grid methods,[8,9] inflation rules,[8] and projection.[10-12] Here, the method of Bak[13] is used, where a periodic set of $(D\text{-}d)$-dimensional "atomic surfaces" in higher (D)-dimensional space is cut appropriately by a d-dimensional hyperplane of physical (parallel) space to produce a quasiperiodic network of points. The atomic surfaces in this work are imbedded in planes that are strictly parallel to the $(D\text{-}d)$ space orthogonal to physical space known as perpendicular space (henceforth called perp. space). For simplicity, this work concerns itself with cuts through structures consisting of a single atomic surface (the "monatomic" case) that is centered at each point of a D-dimensional Bravais lattice, where D is the smallest possible lifting dimension[14] for the symmetry chosen, although many of the results obtained can be generalized for more complicated cases. The Bravais lattices are formed by the integral linear combinations of a set of D basis vectors $\mathbf{e}_i$. The parallel and perp.-space projections of the basis vectors are denoted $\mathbf{e}_i^{\parallel}$ and $\mathbf{e}_i^{\perp}$, respectively. Associated with the atomic surface centered on

$$\mathbf{r}=\sum n_i\mathbf{e}_i+\mathbf{r}_0 \tag{1}$$

are its parallel space component $\mathbf{r}^{\parallel}=\sum n_i\mathbf{e}_i^{\parallel}+\mathbf{r}_0^{\parallel}$ and perp.-space component $\mathbf{r}^{\perp}=\sum n_i\mathbf{e}_i^{\perp}+\mathbf{r}_0^{\perp}$. If $-\mathbf{r}^{\perp}$ is inside the atomic surface, then $\mathbf{r}^{\parallel}$ is projected. Since all atomic surfaces considered here have inversion symmetry, $\mathbf{r}^{\parallel}$ is equivalently projected if $+\mathbf{r}^{\perp}$ is within the atomic surface.

If the volume of the atomic surface is $V_{\perp}$ and the volume of the D-dimensional unit cell is V_D, then the d-dimensional density of projected points is

$$\rho=V_{\perp}/V_D \ . \tag{2}$$

If spheres of radius r are placed around each projected point then the packing fraction f is given by

$$f=\Omega_d r^d\rho \ , \tag{3}$$

where Ω_d is volume of the unit d-dimensional sphere. Maximizing the packing fraction is thus equivalent to maximizing the volume of the atomic surface.

For the sphere packing problem, there is a constraint, namely, the minimum separation constraint, that for spheres of radius r, all pairs of sphere centers must be at least $d_{\min}=2r$ apart. The separation of two projected points is another integral linear combination of parallel space vectors,

$$\Delta\mathbf{r}^{\parallel}=\sum \Delta n_i\mathbf{e}_i^{\parallel} \ . \tag{4}$$

For a given minimum separation constraint, there are an infinite number of possible pair separations of the form (4) that are too close. All such pairs must be avoided for a valid sphere packing. The parallel space condition that no points lie too close together is equivalent to the perp.-space condition that an atomic surface does not contain any pairs of points separated by a perp.-space vector $\Delta\mathbf{r}_x^{\perp}=\sum \Delta n_i\mathbf{e}_i^{\perp}$ whenever $|\Delta\mathbf{r}_x^{\parallel}|<d_{\min}$. The term "constraint vector" will be used henceforth to describe both a parallel space vector that is shorter than $d_{\min}$ and its perp.-space counterpart. The disallowed perp.-space displacements can be sorted in order of increasing perp.-space magnitude. Only the constraint vectors of smallest

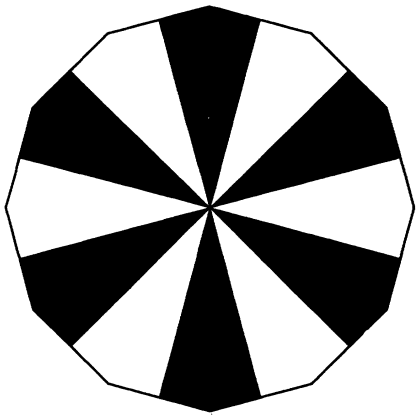

FIG. 1. Example of a pinwheel. The interior of the dodecagonal boundary is the pinwheel region. Half of the pinwheel region is shaded black to indicate that it is part of the atomic surface; the remainder of the pinwheel region is not part of the atomic surface.

perp.-space magnitude play a role in the cases considered here. The perp.-space constraints lead naturally to the construction of connected atomic surfaces such that no point immediately outside the boundary of the atomic surface can be added to the surface without violating the minimum separation constraint. Equivalently, for all points on the boundary of the atomic surface, there are one or more constraint vectors that connect this point with other points on the boundary. Such atomic surfaces will be referred to as "maximal connected surfaces" (MCS). The crux of this paper is to show that under specific conditions, it is possible to replace a MCS by a nonconnected surface of greater volume without violating the minimum separation constraint. The method for creating such atomic surfaces is called the "pinwheel construction" because the nonconnected atomic surfaces contain local regions of high symmetry that typically resemble pinwheels (see Fig. 1). The conditions under which the pinwheel construction can be made are given in the "pinwheel theorem."

The organization of this paper is as follows. Section II describes in detail the pinwheel theorem and the circumstances under which it applies, using the dodecagonal quasicrystal as an example. Section III applies the pinwheel construction to the octagonal case and shows its failure in the decagonal case. In Sec. IV, the pinwheel theorem is shown to apply to an icosahedral packing. The manner in which the pinwheel construction changes the arrangement of spheres in the corresponding projected structure is discussed in Sec. V. Under some circumstances, detailed in Sec. VI, the pinwheel construction can be shown to imply a simple inflation rule for the sphere packing produced. Section VII discusses some other methods for improving the packing fraction of a quasicrystalline sphere packing and Sec. VIII gives a brief summary of the results obtained.

II. THE PINWHEEL THEOREM AND ITS APPLICATION TO DODECAGONAL SPHERE PACKINGS

In this section, the problem of the 12-fold quasicrystalline sphere packing in the plane is considered. To make the terminology consistent throughout this work, "sphere" will be used to refer to a d sphere and, in the context of perp. space, "volume" will be used to refer to a $(D\text{-}d)$-dimensional volume. In the basis used here for dodecagonal quasicrystals,

$$\mathbf{e}_i^{\parallel}=[\cos(2\pi i/12),\sin(2\pi i/12)] \tag{5}$$

and

$$\mathbf{e}_i^{\perp}=[\cos(14\pi i/12),\sin(14\pi i/12)]\ , \tag{6}$$

$0\le i\le 3$, yielding a four-dimensional unit cell volume $V_4=3$. The minimum sphere separation is taken to be 1. Sphere packings in this paper will also be described as the networks formed by the sphere centers (nodes) when joined by linkages which are $d_{\min}$ in length. In all of the structures described in this work, these linkages create a division of parallel space into a number of distinctly shaped regions or "tiles." (Sometimes it proves necessary to include linkages slightly longer than $d_{\min}$ as part of the network in order to yield a tiling.) In the dodecagonal case, the linkages are all of length 1. The maximum density dodecagonal sphere packing is known: the linkages form a tiling of squares and triangles,[15] where the fraction of the plane covered by squares is exactly one-half.[16]

The square-triangle tiling has a density of $(1+2/\sqrt{3})/2\approx 1.0774$ spheres per unit area and yields a packing fraction of $\pi(1+2/\sqrt{3})/8\approx 0.8461$. An infinite number of different packings of this density can be obtained by application of Stampfli's inflation rules.[15] The pinwheel theorem has already been used by Smith to show how atomic surfaces that produce such dense dodecagonal packings can be found.[17] Here the 12-fold packing problem is revisited in more detail so that the general conditions of the pinwheel theorem are made clear.

First, four-dimensional (4D) vectors $\Delta\mathbf{r}_x^{\parallel}$ are found whose parallel space component is less than $d_{\min}$. Then these vectors are sorted in order of increasing $|\Delta\mathbf{r}_x^{\perp}|$. The two sets of constraint vectors with the smallest $|\Delta\mathbf{r}_x^{\perp}|$ are $\{g_i(\mathbf{e}_2^{\parallel}-\mathbf{e}_3^{\parallel})\}$ and $\{g_i(2\mathbf{e}_1^{\parallel}-\mathbf{e}_0^{\parallel}-\mathbf{e}_3^{\parallel})\}$, where $\{g_i\}$ refers to the set of elements of the quasicrystalline point group G (here 12 mm). These sets of vectors have $|\Delta\mathbf{r}_x^{\perp}|=2\cos(\pi/12)\approx 1.9319$ and $|\Delta\mathbf{r}_x^{\perp}|=1+\sqrt{3}\approx 2.7321$, respectively. For quasicrystals with perp.-space dimensionality $D-d=2$, one can use the constraint vectors in a construction akin to the Voronoi construction to find a MCS. First place points at the center of the atomic surface and at all points separated from the center by a constraint vector. Then draw the planes that bisect the line segments connecting the center with the end points of the constraint vectors. Finally, take the region centered at the origin entirely within these bisectors to be the atomic surface. For the 12-fold case, only the bisectors of the set of vectors $\{g_i(\mathbf{e}_2^{\perp}-\mathbf{e}_3^{\perp})\}$ contribute to the boundary of the MCS, which is a regular dodecagon of maximum radius 1 along the directions $\{g_i(\mathbf{e}_0^{\perp})\}$. It is convenient to define a function $f(\mathbf{r}^{\perp})$ such that $f(\mathbf{r}^{\perp})=1$ if $\mathbf{r}^{\perp}$ is in the atomic surface and $f(\mathbf{r}^{\perp})=0$ if $\mathbf{r}^{\perp}$ is outside the atomic surface. The MCS for a $D-d=2$ quasicrystal is then given by $f(\mathbf{r}^{\perp})=1$ if

$$\mathbf{r}^{\perp}\cdot\Delta\mathbf{r}_x^{\perp}<|\Delta\mathbf{r}_x^{\perp}|^2/2 \tag{7}$$

for all $\Delta\mathbf{r}_x^\perp$ and $f(\mathbf{r}^\perp)=0$ if

$$\mathbf{r}^\perp\cdot\Delta\mathbf{r}_x^\perp > |\Delta\mathbf{r}_x^\perp|^2/2 \tag{8}$$

for any $\Delta\mathbf{r}_x^\perp$. The problem of giving $f(\mathbf{r}^\perp)$ a value on the boundary of the atomic surface will be ignored in this work, since, in practice, one can choose $\mathbf{r}_0$ in Eq. (1) so as to avoid projecting boundary points. However, whether an atomic surface that contains regions of finite size that only meet at a finite number of points is connected does depend on how $f(\mathbf{r}^\perp)$ is defined at the points that they meet. Throughout this work, such a surface will be considered as nonconnected.

If $\mathbf{r}^\perp$ is on the boundary of the atomic surface, then $\mathbf{r}^\perp\cdot\Delta\mathbf{r}_x^\perp=|\Delta\mathbf{r}_x^\perp|^2/2$ for one or more $\Delta\mathbf{r}_x^\perp$. One immediately has $(\mathbf{r}^\perp-\Delta\mathbf{r}_x^\perp)\cdot\Delta\mathbf{r}_x^\perp=-|\Delta\mathbf{r}_x^\perp|^2/2$. Since each point on the boundary is displaced from at least one other point on the boundary by a constraint vector, the surface is proven to be a MCS. Furthermore, the displacement of any point inside the MCS by any $\Delta\mathbf{r}_x^\perp$ violates Eq. (7) and is outside the MCS, and thus the MCS gives a valid sphere packing. Despite the fact that the dodecagonal-shaped atomic surface is maximal, its volume is only $V_\perp(\text{MCS})=3$ giving a density of projected points $\rho=1$, less than that for the square-triangle tiling. Figure 2(d) shows a region of the network generated by the dodecagonal MCS. Note that it contains distorted hexagons which reduce the density from that of the square-triangle tiling.

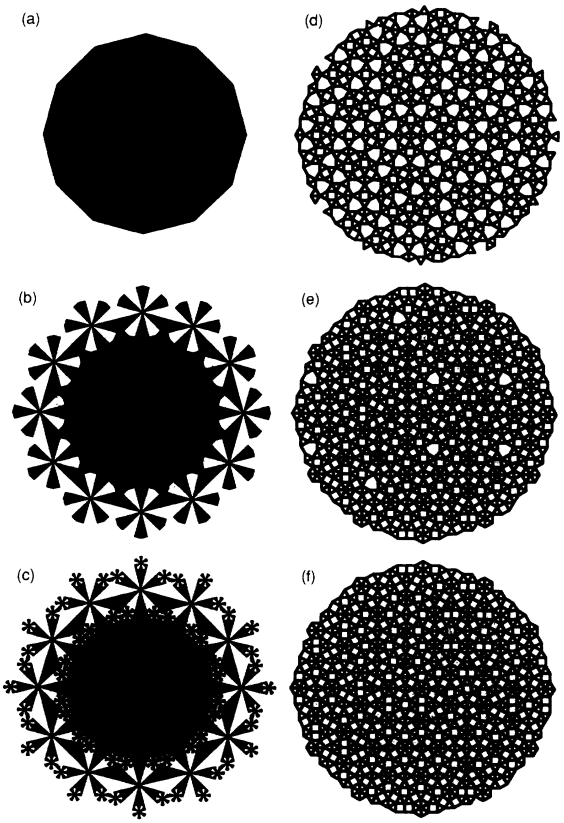

FIG. 2. (a)–(c) The MCS for the dodecagonal sphere packing problem and the atomic surfaces for the first two stages of the iterated pinwheel construction. (d)–(f) The tilings corresponding to the projections of the surfaces shown in (a)–(c), respectively.

A set of special points for the pinwheel construction can now be found. The set of special points $\{\mathbf{r}_s\}$ must possess the following properties. (S1) All special points are on the boundary of the atomic surface. (S2) The set of special points is a single orbit of the point group G of the atomic surface. (S3) Every point on the boundary of the atomic surface that is separated from a special point by a constraint vector must also be a special point. (S4) There must be at least two other special points connected to each special point via constraint vectors. (S5) The MCS must be "convex" at each special point, that is, the filling fraction about $\mathbf{r}_s^\perp, p(\mathbf{r}_s^\perp)$, must satisfy

$$p(\mathbf{r}_s^\perp)=\lim_{\delta r_0^\perp\to 0}\frac{\int_{|\delta\mathbf{r}^\perp|<\delta r_0^\perp} dV_\perp f(\mathbf{r}_s^\perp+\delta\mathbf{r}^\perp)}{\int_{|\delta\mathbf{r}^\perp|<\delta r_0^\perp} dV_\perp} < \frac{1}{2}\ . \tag{9}$$

If one connects each special point with the other special points that are separated from it by constraint vectors, one obtains a network or networks of special points. In the case where there is more than one network, the networks will be distinguished by being labeled $\{\mathbf{r}_{si}^\perp\}$. The subscript "$i$" will be omitted when there is only a single network. The pinwheel theorem can now be stated: If the network or each individual network of special points of a maximal connected atomic surface has no loops containing an odd number of links, then it is possible to increase the volume of the atomic surface without violating minimum separation constraints by replacing it with a nonconnected atomic surface.

The pinwheel construction is accomplished by changing the atomic surface within a volume S_{ij} centered on each special point $\mathbf{r}_{sij}^\perp$. These regions, $\{\mathbf{r}_{sij}^\perp+\delta\mathbf{r}_{ij}^\perp\}$, $\delta\mathbf{r}_{ij}^\perp\in S_{ij}$ will be referred to as the pinwheel regions. The volumes $\{S_{ij}\}$ must have the following properties. (P1) Each S_{ij} has the symmetry G_i where G_i is the subgroup of G that leaves the ith network of special points $\mathbf{r}_{si}^\perp$ invariant. (P2) Each S_{ij} centered on a special point $\mathbf{r}_{si}^\perp$ in the same network is identical. (P3) Pinwheel regions about special points on different networks are related by symmetry: $S_{kl}=g_k(S_{ij})$, where g_k is such that $g_k(\mathbf{r}_{sij}^\perp)=\mathbf{r}_{skl}^\perp$. (P4) Pinwheel regions do not overlap. If $\mathbf{r}_{sij}^\perp\neq\mathbf{r}_{skl}^\perp$ then for all $\delta\mathbf{r}_{ij}^\perp\in S_{ij}$ and $\delta\mathbf{r}_{kl}^\perp\in S_{kl}$,

$$\mathbf{r}_{sij}^\perp+\delta\mathbf{r}_{ij}^\perp\neq\mathbf{r}_{skl}^\perp+\delta\mathbf{r}_{kl}^\perp\ . \tag{10}$$

(P5) No new constraint vectors are introduced between pinwheel regions. If $\mathbf{r}_{sij}^\perp\neq\mathbf{r}_{skl}^\perp$ and $\delta\mathbf{r}_{ij}^\perp\in S_{ij}$ and $\delta\mathbf{r}_{kl}^\perp\in S_{kl}$ then

$$\mathbf{r}_{sij}^\perp+\delta\mathbf{r}_{ij}^\perp+\Delta\mathbf{r}_x^\perp\neq\mathbf{r}_{skl}^\perp+\delta\mathbf{r}_{kl} \tag{11}$$

unless $\mathbf{r}_{sij}^\perp+\Delta\mathbf{r}_x^\perp=\mathbf{r}_{skl}^\perp$.

Constraints (P4) and (P5) lead to a natural definition for the boundaries of a connected pinwheel region of maximum volume. Define a set of effective constraint vectors

$$\{\Delta\mathbf{r}_{xij}^\perp\}\equiv(\{\mathbf{r}_{kl}^\perp-\mathbf{r}_{ij}^\perp\}\cup\{\mathbf{r}_{kl}^\perp+\Delta\mathbf{r}_x^\perp-\mathbf{r}_{ij}^\perp\})\cap\mathbf{0}\ . \tag{12}$$

Then the following pinwheel regions will satisfy constraints (P4) and (P5): $\delta\mathbf{r}_{ij}^\perp\in S_i$ if

$$\delta\mathbf{r}_{ij}^{\perp}\cdot g_{ik}(\Delta\mathbf{r}_{xij}^{\perp})<\tfrac{1}{2}|\Delta\mathbf{r}_{xij}^{\perp}|^2 \tag{13}$$

for all $\Delta\mathbf{r}_{xij}^{\perp}$ and $g_{ik}\in G_i$.

Half the volume of each pinwheel region is then filled in a manner that preserves the symmetry G of the atomic surface and that introduces no pairs of atoms that violate the minimum separation constraint. This "pinwheel construction" is accomplished as follows. Pick an arbitrary special point $\mathbf{r}_{ij}^{\perp}$. Since the network of special points that this point is on has no odd-length loops, it is bipartite. Call the subnetwork that $\mathbf{r}_{ij}^{\perp}$ is on the even-parity subnetwork of $i\{\mathbf{r}_{sie}^{\perp}\}$. Call the other subnetwork the odd-parity subnetwork $\{\mathbf{r}_{sio}^{\perp}\}$. Define S_{iw} to be an irreducible wedge of S_i. Then,

$$f(\{\mathbf{r}_{sie}^{\perp}\}+\delta\mathbf{r}^{\perp}),\quad \delta\mathbf{r}^{\perp}\in S_{iw} \tag{14}$$

can be chosen to be any function that takes on the value 0 or 1 at each point. The value of f within the remainder of the pinwheel regions is given by the following. Define a parity operator P such that $P(g_{ij})=0$ if $g_{ij}(\{\mathbf{r}_{sie}^{\perp}\})=\{\mathbf{r}_{sie}^{\perp}\}$ and $P(g_{ij})=1$ if $g_{ij}(\{\mathbf{r}_{sie}^{\perp}\})=\{\mathbf{r}_{sio}^{\perp}\}$. Then

$$f[g_{ik}(\mathbf{r}_{ij}^{\perp})+g_{il}(\delta\mathbf{r}^{\perp})]=f(\mathbf{r}_{ij}^{\perp}+\delta\mathbf{r}^{\perp}) \tag{15}$$

if $P(g_{ik})=P(g_{il})$, otherwise,

$$f[g_{ik}(\mathbf{r}_{ij}^{\perp})+g_{il}(\delta\mathbf{r}^{\perp})]=1-f(\mathbf{r}_{ij}^{\perp}+\delta\mathbf{r}^{\perp})\ . \tag{16}$$

The value of f within pinwheel regions on the other networks is given by

$$f[g_k(\{\mathbf{r}_{si}^{\perp}\}+\delta\mathbf{r}^{\perp})]=f(\{\mathbf{r}_{si}^{\perp}\}+\delta\mathbf{r}^{\perp})\ . \tag{17}$$

Note that this construction introduces no pairs that violate the minimum separation constraint, since

$$f(\mathbf{r}_s^{\perp}+\delta\mathbf{r}^{\perp}+\Delta\mathbf{r}_x^{\perp})=0 \tag{18}$$

if $\mathbf{r}_s^{\perp}+\Delta\mathbf{r}_x^{\perp}\notin\{\mathbf{r}_s^{\perp}\}$, by constraint (P5) and

$$f(\mathbf{r}_s^{\perp}+\delta\mathbf{r}^{\perp}+\Delta\mathbf{r}_x^{\perp})=1-f(\mathbf{r}_s^{\perp}+\delta r^{\perp}) \tag{19}$$

if $\mathbf{r}_s^{\perp}+\Delta\mathbf{r}_x^{\perp}\in\{\mathbf{r}_s^{\perp}\}$ according to Eq. (16) and the fact that constraint vectors always connect special points of opposite parity. Note also that, while before the pinwheel construction the fraction of each pinwheel region S_{ij} filled is less than one-half because of condition (S5), after the pinwheel construction, each S_{ij} is one-half filled. Thus, the pinwheel construction increases the volume of the atomic surface and the density of the corresponding sphere packing.

As an example, the pinwheel construction for the dodecagonal quasicrystal with symmetry 12 mm will now be derived in detail. The MCS for this case has already been determined. The only points on the boundary of the MCS that satisfy (S5) are the corners of the MCS, $\{g_i(\mathbf{e}_0^{\perp})\}$. These points satisfy all of the other special point conditions and are thus the unique set of special points for the MCS. Each special point is linked to two others by constraint vectors; a network of length 12 is formed. The network is bipartite and thus the 12 mm MCS satisfies the pinwheel theorem and can be expanded. The special points and the network formed are shown in Fig. 3.

The maximum connected pinwheel region about each special point is determined by the effective constraint vectors

$$\{g_i(\Delta\mathbf{r}_{xj}^{\perp})\}=\{g_i(2\mathbf{e}_0^{\perp}+2\mathbf{e}_1^{\perp}-\mathbf{e}_3^{\perp})\}\ .$$

The pinwheel regions that satisfy Eq. (13) are dodecagons that have diameters $1/(2+\sqrt{3})$ that of the original MCS and are shown in Fig. 4. Note that pinwheel regions about adjacent special points touch without overlapping.

The two generators of 12 mm, $R_{\pi/6}$, and reflection through the $\mathbf{e}_0^{\perp}+\mathbf{e}_3^{\perp}$ axis, both move special points into those of the opposite parity. One can use this in conjunction with Eqs. (14)–(16) to construct a symmetry-preserving pinwheel. It is natural to choose $f(\{\mathbf{r}_e^{\perp}\}+\delta\mathbf{r}^{\perp})=1$ for all $\delta\mathbf{r}^{\perp}\in S_{iw}$. This choice for filling the irreducible wedge produces shapes that resemble pinwheels for which the pinwheel theorem is named (see Fig. 1), although other fillings of the irreducible wedge are possible which do not produce pinwheel-like shapes [see Fig. 5(b)].

The volume of the new atomic surface, shown in Fig. 2(b), is

$$V_{\perp 1}=V_{\perp}(\mathrm{MCS})+12\left[\frac{1}{2}-\frac{5}{12}\right]\frac{V_{\perp}(\mathrm{MCS})}{(2+\sqrt{3})^2}$$
$$=\frac{8+4\sqrt{3}}{7+4\sqrt{3}}V_{\perp}(\mathrm{MCS})\ , \tag{20}$$

which leads to a node density of $V_{\perp 1}/3\approx 1.0718$ which is still less than that of the square-triangle tiling.

However, there is no reason to assume that the individual pinwheel regions themselves must be connected. Under some conditions, the atomic surface volume can be further expanded by use of nonconnected pinwheel regions. These conditions are established by the following

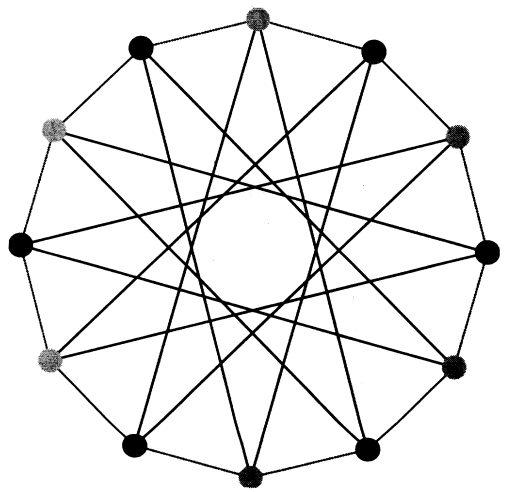

FIG. 3. Special points of the dodecagonal MCS and the network that they form. The special points are indicated by circles. The interior lines are the constraint vectors that form the links of the network. The two colorings of the special points indicate how the network is bipartite.

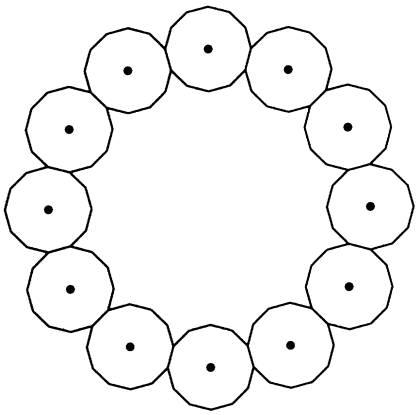

FIG. 4. Special points of the dodecagonal MCS and the dodecagon-shaped pinwheel region surrounding each special point.

generalization of the pinwheel theorem. In the same way special points were found before, find points on the boundary of the pinwheel regions that satisfy the following conditions. (N1) The set of special points on the boundary of a given pinwheel region is a single orbit of the point group G_i of the pinwheel region. (N2) New special points on the boundary of other pinwheel regions must be related to those of a given pinwheel region by symmetry. (N3) Connect the new special points by the constraint vectors that connect the centers of the pinwheel regions to which they belong. These networks of new special points must contain new special points that are "linked" to new special points on at least two other networks of new special points either by constraint vectors or by coincidence. (N4) The pinwheel region must be "convex" about each new special point in a manner analogous to condition (S5) for the special points.

For each such new special point, form the network of new special points described in condition (N3). Then, determine the "supernetworks" of the networks of new special points where two networks are linked if there is any constraint vector that connects a special point on one network with one on the other or if they contain new special points that are separated by a constraint vector. Now, if the supernetwork is bipartite in the manner of the pinwheel theorem, then the pinwheel construction can be performed anew on the new special points. The proof is similar to that for the pinwheel theorem. For the dodecagonal case considered, the new special points are the 144 points, 120 of which are distinct, on the corners of the pinwheel regions surrounding the old special points, specifically $\{g_i(\mathbf{e}_0^\perp)\}+\{g_j(2\mathbf{e}_0^\perp+2\mathbf{e}_1^\perp-\mathbf{e}_3^\perp)\}$. These form 12 networks which form a supernetwork whose links are between networks that share points, e.g., the points indicated by the largest circles in Fig. 6. This supernetwork is bipartite and thus new pinwheel regions can be grown around the new special points to increase the atomic surface volume further. The size of these new pinwheel regions are limited by effective constraint vectors in a manner similar to that which limits the pinwheel regions, Eq. (13). Note that the new pinwheel region about each new special point fills only half the surround-

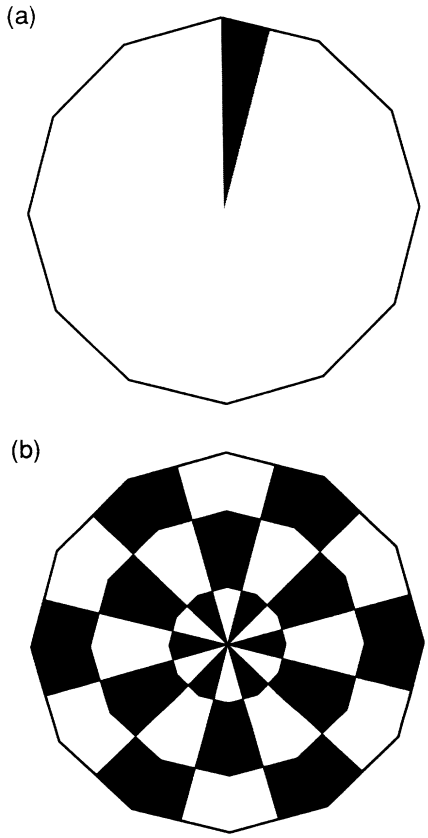

FIG. 5. (a) Pinwheel region from Fig. 4 showing the irreducible wedge of symmetry 12 mm. (b) Alternate decoration of the pinwheel region. The decorations shown in Fig. 1 and in (b) both produce valid sphere packings when they are used to fill the pinwheel regions about the even special points and the rotation of the decorations by $\pi/12$ are used to fill the pinwheel regions about the odd special points.

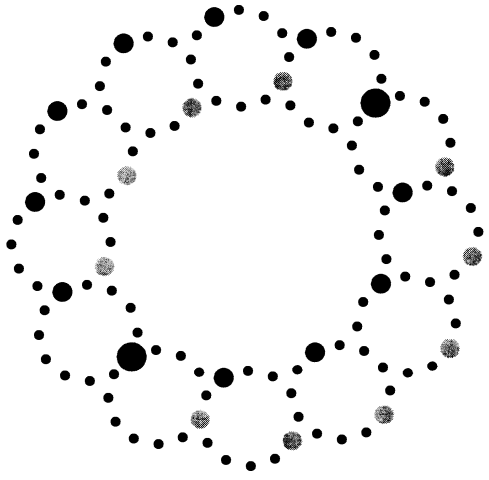

FIG. 6. New special points for the second stage of the iterated pinwheel construction for dodecagonal symmetry. The medium gray circles indicate new special points on one network like that in Fig. 3; the large solid circles indicate special points on another network. The two networks share the points indicated by the largest solid circles and thus are linked in the supernetwork of such networks.

ing volume due to the supernetwork constraints, and furthermore, only half of these regions are filled due to the network constraints. An atomic surface for dodecagonal symmetry with the new pinwheel regions filled is shown in Fig. 2(c).

In a similar manner, after maximizing the new pinwheels, it may be possible to further extend the volume of the atomic surface by performing the pinwheel construction on yet another set of special points. This procedure will be called the iterated pinwheel construction.

In the dodecagonal case, the iterated pinwheel construction is particularly easy to follow, because each step involves pinwheel construction about a set of new special points that are the vertices of dodecagons centered on the old special points, oriented in the same way and with a radius $1/(2+\sqrt{3})$ that of the dodecagons that formed the old special points. The volume of the atomic surface at each stage of the pinwheel construction can be determined by noting that the pinwheel region in each step is similar in shape to and of linear dimension $1/(2+\sqrt{3})$ that of the entire atomic surface of the previous step:

$$V_{\perp(n+1)}=V_{\perp}(\mathrm{MCS})+12\left[\frac{1}{2}-\frac{5}{12}\right]\frac{V_{\perp n}}{(2+\sqrt{3})^2}\ . \tag{21}$$

After infinitely many iterations,

$$V_{\perp}=\left[\frac{1}{2}+\frac{\sqrt{3}}{3}\right]V_{\perp}(\mathrm{MCS})\ . \tag{22}$$

The density of points obtained is exactly that of the square-triangle tiling. Next one must check that the procedure has not introduced any new constraint vectors. The constraint vectors of length $1+\sqrt{3}$ do not occur within the new atomic surface because the maximum radius of the atomic surface is

$$r=\sum_{n=0}^{\infty}\frac{1}{(2+\sqrt{3})^n}=(1+\sqrt{3})/2\ . \tag{23}$$

The atomic surface just barely avoids containing points separated by this set of constraint vectors. All other constraint vectors have $|\mathbf{r}^{\perp}|$ even larger and so are not contained within the surface. Thus, the infinitely iterated limit of the pinwheel construction must *be* a square-triangle tiling. Note that Fig. 2(f), which shows a portion of the tiling corresponding to only the second iteration of the pinwheel construction, already contains only squares and triangles over regions as large as the approximately 700-tile region shown. It is clear by the nature of the construction that the final atomic surface is a fractal, as has been noted previously.[18,19] The choices for filling the pinwheel regions used in Figs. 2(b) and 2(c), in the infinitely iterated limit, produce an atomic surface shape apparently identical to that found by Baake.[18] By using other choices for filling the pinwheel regions at each stage of the iterated pinwheel construction, it is possible to achieve the same maximum density with an infinite number of differently shaped atomic surfaces.

III. OCTAGONAL AND DECAGONAL SPHERE PACKINGS

Now, the pinwheel theorem will be applied to the octagonal and decagonal sphere packing problems. For the octagonal case, the basis vectors used are

$$\mathbf{e}_i^{\parallel}=[\cos(2\pi i/8),\sin(2\pi i/8)] \tag{24}$$

and

$$\mathbf{e}_i^{\perp}=[\cos(10\pi i/8),\sin(10\pi i/8)]\ . \tag{25}$$

For the decagonal case, the basis vectors used are

$$\mathbf{e}_i^{\parallel}=[\cos(4\pi i/10),\sin(4\pi i/10)] \tag{26}$$

and

$$\mathbf{e}_i^{\perp}=[\cos(8\pi i/10),\sin(8\pi i/10)]\ . \tag{27}$$

In each case $0\le i\le 3$. These give $V_4=4$ for the octagonal case and $V_4=5^{3/2}/4\approx 2.7951$ for the decagonal case.

First consider the octagonal case. The three sets of constraint vectors with the smallest $|\Delta\mathbf{r}_x^{\perp}|$ are $\{g_i(\mathbf{e}_2^{\parallel}-\mathbf{e}_3^{\parallel})\}$, $\{g_i(\mathbf{e}_1^{\parallel}-\mathbf{e}_0^{\parallel}-\mathbf{e}_3^{\parallel})\}$, and $\{g_i(2\mathbf{e}_0^{\parallel}+\mathbf{e}_3^{\parallel}-\mathbf{e}_1^{\parallel})\}$, with $|\Delta\mathbf{r}_x^{\perp}|=2\cos(\pi/8)\approx 1.8478$, $|\Delta\mathbf{r}_x^{\perp}|=1+\sqrt{2}\approx 2.4142$, and $|\Delta\mathbf{r}_x^{\perp}|=2+\sqrt{2}\approx 3.4142$, respectively. The MCS is formed by the perpendicular bisectors of the set of vectors with the smallest $|\Delta\mathbf{r}_x^{\perp}|$ and is shaped like an octagon with largest radius 1. The volume is $V_{\perp}(\mathrm{MCS})=2\sqrt{2}$. The corners of the octagon, $\{g_i(\mathbf{e}_0)\}$, are special points and form a bipartite network. Therefore, the pinwheel construction can be performed at each special point. The size of the pinwheels are limited in this case by the second shortest set of constraint vectors. Pinwheel regions may be extended out to octagons whose radius is $[(\sqrt{2}-1)/2]/\cos(\pi/8)$ that of the MCS and which are oriented at a $\pi/8$ rotation with respect to the orientation of the MCS. It is possible to iterate the pinwheel construction. The new special points are the corners of the small octagons. Each subsequent iteration constructs octagons of radius $\sqrt{2}-1$ that of the previous iteration, centered on the vertices of the octagons of the previous iteration and oriented in the same direction. The final atomic surface is again a fractal as it was for the dodecagonal case.[20] The volume of the surface is $V_{\perp}=3$, yielding $\rho=0.75$ or $f=3\pi/16\approx 0.5890$, a rather poor packing fraction. The final atomic surface extends beyond the Voronoi domain associated with the second shortest set of constraint vectors, in violation of an earlier assumption that this domain confines the pinwheel regions.[17]

The atomic surfaces and sections of the tilings for the MCS and the first two steps of the iterated pinwheel construction are shown in Figs. 7(a)–7(f). The tiles included are squares, flattened hexagons, regular octagons, concave octagons, and the tile with 10 boundary points and one interior point. It is likely that a denser packing involving the same linkages exists. It is possible to put an upper bound on the node density. The two tiles with highest node density are the square and flattened hexagon. Squares by themselves are obviously insufficient to

tile the plane with octagonal symmetry, so both squares and (at least) hexagons are necessary. A hexagon can be divided into a square and two 45° rhombii as shown in Fig. 8. It is easy to show using the grid method[21] that for a tiling consisting of squares and 45° rhombii to have octagonal symmetry, the ratio of squares to rhombii must be $n_S:n_R=1:\sqrt{2}$. If the packing is done using only squares and hexagons, then the corresponding ratio of squares to hexagons must be $n_S:n_H=1:1+\sqrt{2}$. The density of nodes is thus

$$\tfrac{1}{4}(2+\sqrt{2})\approx 0.8536\ . \tag{28}$$

This upper limit on the density is significantly higher than that found by the pinwheel construction. However, there are no known octagonal tilings consisting solely of squares and hexagons. Finding the maximum density octagonal sphere packing with linkages of length 1 in a set of octagonal directions remains an interesting unsolved problem. The octagonal case has implications for icosahedral tiling models. These implications will be discussed in Sec. IV.

In the decagonal case, the three sets of constraint vectors with the smallest $|\Delta\mathbf{r}_x^\perp|$ are $\{g_i(-\mathbf{e}_0^\parallel-\mathbf{e}_2^\parallel-\mathbf{e}_3^\parallel)\}$, $\{g_i(2\mathbf{e}_0^\parallel+\mathbf{e}_2^\parallel+\mathbf{e}_3^\parallel)\}$, and $\{g_i(\mathbf{e}_0^\parallel-\mathbf{e}_1^\parallel+\mathbf{e}_2^\parallel-\mathbf{e}_3^\parallel)\}$ with $|\Delta\mathbf{r}_x^\perp|=\tau\approx 1.6180$, $|\Delta\mathbf{r}_x^\perp|=\tau^2\approx 2.6180$, and $|\Delta\mathbf{r}_x^\perp|=\sqrt{\tau^3/s}\approx 3.0777$, respectively, where $s\equiv 1/\sqrt{5}$ and τ is the golden mean, $\tau=(1+\sqrt{5})/2$. The MCS is a decagon of largest radius $\sqrt{s\tau}\approx 0.8507$. The corners of the decagon are in directions that are the basis vector directions rotated by $\pi/10$. The MCS has an area of $V_\perp=5\sqrt{s\tau}/2$ which corresponds to a density of projected points $\rho=10\sqrt{s^7\tau}\approx 0.7608$ and a packing fraction of $f=5\pi\sqrt{s^7\tau}/2\approx 0.5976$. The MCS and a portion of the corresponding tiling is shown in Figs. 9(a) and 9(c). The corners of the MCS, $\{g_i(2\mathbf{e}_0^\perp-\mathbf{e}_1^\perp+\mathbf{e}_2^\perp-2\mathbf{e}_3^\perp)/5\}$, are special points; however, they link to form two networks of length 5. Both networks have an odd number of links and thus are not bipartite. Therefore, the pinwheel theorem does not apply to this decagonal case. More will be said about the decagonal sphere packing problem in Sec. VII.

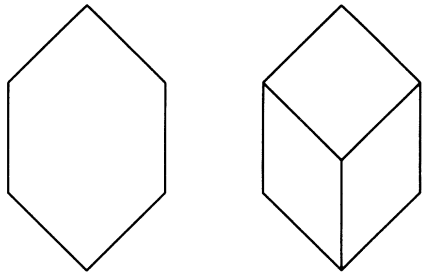

FIG. 8. Division of a flattened hexagon into a square and two rhombii.

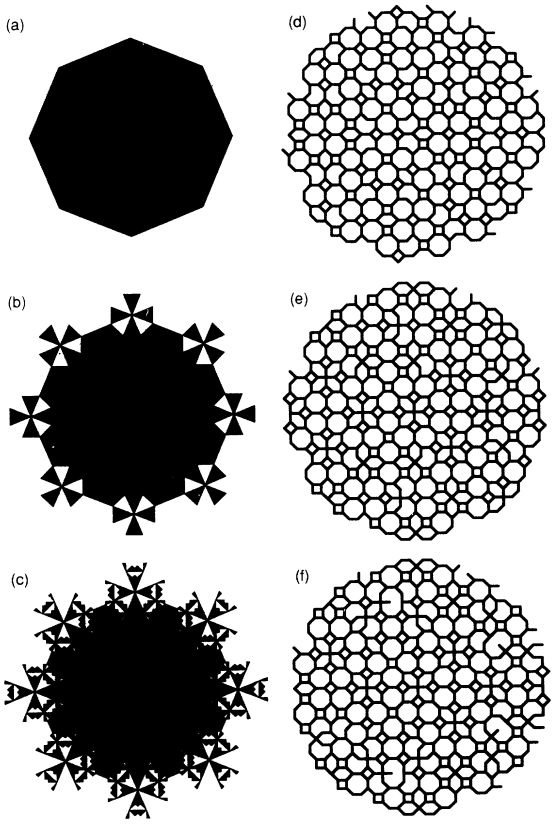

FIG. 7. (a)–(c) The MCS for the octagonal sphere packing problem and the atomic surfaces for the first two stages of the iterated pinwheel construction. (d)–(f) The tilings corresponding to the projections of the surfaces shown in (a)–(c), respectively.

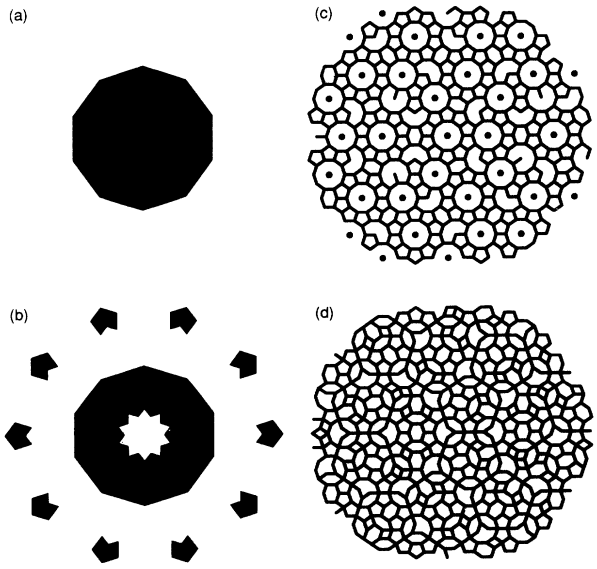

FIG. 9. (a) and (b) The MCS for the decagonal sphere packing problem and a nonconnected atomic surface for this problem. (c) and (d) The tilings corresponding to the projections of the surfaces shown in (a) and (b), respectively.

IV. ICOSAHEDRAL SPHERE PACKINGS

The icosahedral sphere packing problem is of great interest because of the existence of intermetallic alloys with icosahedral symmetry.[22] Two separate icosahedral sphere packing problems are examined in this section. First, the icosahedral sphere packing problem with $d_{\min}=1$ is considered and it is found that the pinwheel theorem does not apply. Next, the icosahedral sphere packing problem with $d_{\min}=\sqrt{3s/\tau^3}\approx 0.5628$ is investigated and it is found that the packing fraction of the MCS can be improved via the pinwheel construction.

For icosahedral symmetry, $D=6$, $D-d=3$, and the six-dimensional lattice is cubic. The basis used here is

$$\begin{aligned}
\mathbf{e}_0&=\eta(0,\tau,1,0,-1,\tau)\ ,\\
\mathbf{e}_1&=\eta(1,0,\tau,\tau,0,-1)\ ,\\
\mathbf{e}_2&=\eta(\tau,1,0,-1,\tau,0)\ ,\\
\mathbf{e}_3&=\eta(0,\tau,-1,0,-1,-\tau)\ ,\\
\mathbf{e}_4&=\eta(-\tau,1,0,1,\tau,0)\ ,
\end{aligned}\tag{29}$$

and

$$\mathbf{e}_5=\eta(-1,0,\tau,-\tau,0,-1)\ .$$

The constant η is equal to $(\sqrt{5}\tau)^{-1/2}$ and the components are given in the form $(\mathbf{e}_i^{\parallel},\mathbf{e}_i^{\perp})$. The six-dimensional unit cell has volume $V_6=8$.

To use the pinwheel theorem, it is first necessary to generate a MCS. The technique given in Sec. II for generating the MCS's of planar quasicrystals fails for the icosahedral problems considered in this section. Still, atomic surfaces for icosahedral quasicrystals that satisfy the MCS conditions have been found. They will be used here without reporting methods for their derivations or proof that they are unique.

When $d_{\min}=1$, the MCS is the truncated stellated dodecahedron[23] shown in Fig. 10. It has a volume of

$$V_{\perp}(\mathrm{MCS})=\frac{240\tau^4+140\tau^3}{(16\tau+12)^{3/2}}\tag{30}$$

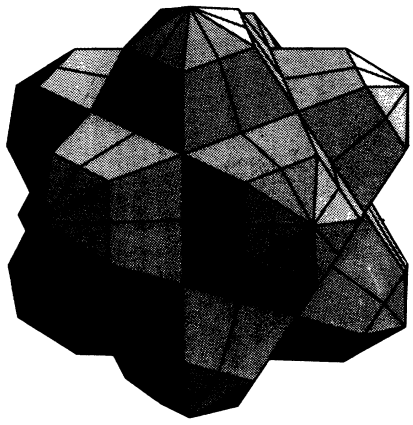

FIG. 10. Truncated stellated dodecahedron atomic surface for the $d_{\min}=1$ icosahedral sphere packing problem.

and the packing fraction of the corresponding projected structure is

$$f=\frac{\pi}{12}\frac{60\tau^4+35\tau^3}{(16\tau+12)^{3/2}}\approx 0.6281\ .\tag{31}$$

The two shortest linkages in the projected structures are those of length 1 along icosahedral fivefold directions and those of length $2\sqrt{s/\tau}\approx 1.0515$ $(s\equiv 1/\sqrt{5})$ along icosahedral twofold directions. Denoting icosahedral fivefold, twofold, and threefold directions by the letters "*a*," "*b*," and "*c*," respectively, the projected structure is an example of an icosahedral *a*-*b* network.

The sets of constraint vectors that connect points on the boundary of the MCS are $\mathbf{r}_x^{\perp}=\{g_i(\mathbf{e}_3^{\perp}-\mathbf{e}_4^{\perp}+\mathbf{e}_5^{\perp})\}$ along icosahedral threefold directions with $|\Delta\mathbf{r}_x^{\perp}|=\sqrt{3s\tau^3}\approx 2.3840$ and $\mathbf{r}_x^{\perp}=\{g_i(\mathbf{e}_0^{\perp}+\mathbf{e}_1^{\perp}-\mathbf{e}_2^{\perp}-\mathbf{e}_5^{\perp})\}$ along icosahedral twofold directions with $|\Delta\mathbf{r}_x^{\perp}|=2\sqrt{s\tau^3}\approx 2.7528$.

There is one set of special points and a related family of sets of special points for the $d_{\min}=1$ MCS. The first set of special points is

$$\{g_i[(-\mathbf{e}_0^{\perp}+\mathbf{e}_1^{\perp}+\mathbf{e}_2^{\perp}+\mathbf{e}_3^{\perp}+\mathbf{e}_4^{\perp}+\mathbf{e}_5^{\perp})/2]\}\ .\tag{32}$$

These special points lie on the 12 fivefold vertices of the MCS shown in Fig. 10 and they form a network that contains both 3-loops and 5-loops. Therefore, the pinwheel construction is not possible on these special points. The family of sets of special points is

$$\{g_i[(-\mathbf{e}_0^{\perp}+\mathbf{e}_1^{\perp}+\mathbf{e}_2^{\perp}+\mathbf{e}_3^{\perp}+\mathbf{e}_4^{\perp}+\mathbf{e}_5^{\perp})/2-\lambda\mathbf{e}_2^{\perp}]\}\ ,\qquad 0<\lambda<\tau^{-1}\ .\tag{33}$$

Each special point in this family lies on an edge of the MCS shown in Fig. 10 that connects a fivefold vertex with a corner of the surrounding pentagon. Each set of special points in the family contains 60 special points which break down into 12 networks that are loops of length 5. Since the loop size is again odd, these sets of special points also do not allow pinwheel constructions. The pinwheel construction is thus impossible on the MCS used for the $d_{\min}=1$ icosahedral sphere packing problem.

The MCS for the $d_{\min}=\sqrt{3s/\tau^3}$ sphere packing problem is a "ruffled" truncated triacontahedron[24] and is shown in Fig. 11. The sets of constraint vectors that connect points on the boundary of this MCS are

$$\mathbf{r}_x^{\perp}=\{g_i(-2\mathbf{e}_0^{\perp}+\mathbf{e}_1^{\perp}+\mathbf{e}_2^{\perp}+\mathbf{e}_3^{\perp}+\mathbf{e}_4^{\perp}+\mathbf{e}_5^{\perp})\}$$

along icosahedral fivefold directions with $|\Delta\mathbf{r}_x^{\perp}|=\tau^3\approx 4.2361$ and

$$\mathbf{r}_x^{\perp}=\{g_i(-\mathbf{e}_0^{\perp}-\mathbf{e}_1^{\perp}+2\mathbf{e}_2^{\perp}+2\mathbf{e}_5^{\perp})\}$$

along icosahedral twofold directions with $|\Delta\mathbf{r}_x^{\perp}|=2\sqrt{s\tau^5}\approx 4.4541$. The volume of this MCS is $V_{\perp}=20s^{3/2}\tau^{9/2}(1-\tau^{-5})$ and the corresponding packing fraction is

$$f=\frac{\pi}{2}\left[\frac{3}{4}\right]^{1/2}s(1-\tau^{-5})\approx 0.5535\ .\tag{34}$$

The shortest linkages in parallel space are $d_{\min}$ along icosahedral threefold directions and $2\sqrt{s/\tau^3}\approx 0.6498$

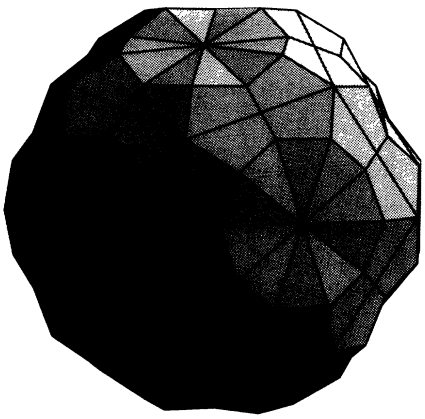

FIG. 11. Truncated triacontahedron atomic surface for the $d_{\min} \approx 0.5628$ icosahedral sphere packing problem.

along icosahedral twofold directions, thus the structure is an example of an icosahedral *b-c* network. The linkages multiplied by $\tau^3 a$, a the quasilattice constant,[11] are the same linkages that connect clusters in cluster-based models of the icosahedral phase such as Henley's canonical cell model.[25] The sphere packing problem is hence equivalent to the cluster packing problem. The highest-density sphere packing corresponds with the highest density cluster packing. Random aggregation studies[26,27] suggest a packing fraction of 0.60 to 0.61 is possible for this problem, well above the packing fraction of the MCS. Mihalkovič and Mrafko[28] have generated large-unit-cell periodic approximants consisting entirely of canonical cells, which also suggest a packing fraction of 0.60 to 0.61 is possible.

The MCS for the $d_{\min} \approx 0.5628$ sphere packing problem has the following sets of special points. (1) The set $\{g_i(\mathbf{e}_3^\perp - \mathbf{e}_4^\perp + \mathbf{e}_5^\perp)\}$ having 20 vertices on the regular dodecahedron formed by the threefold vertices of the MCS shown in Fig. 11. In this case, the special points form a network that contains 3-loops and 5-loops which makes the pinwheel construction impossible. (2) The family of sets $\{g_i(\mathbf{e}_3^\perp - \mathbf{e}_4^\perp + \mathbf{e}_5^\perp + \lambda \mathbf{e}_1^\perp)\}$, $0 < \lambda < \tau^{-1}$, each containing 60 special points on the edges of the MCS in Fig. 11 that connect threefold vertices with vertices on ruffled decagons. These special points form 12 networks that are loops of length 5. Again the pinwheel construction is impossible. (3) The set $\{g_i(\mathbf{e}_0^\perp - \mathbf{e}_1^\perp + 2\mathbf{e}_2^\perp - 2\mathbf{e}_3^\perp + \mathbf{e}_4^\perp)/2\}$ consisting of 120 special points which are located on the centers of each of the edges of the ruffled decagons of the MCS shown in Fig. 11. These edges are along icosahedral threefold directions. These special points form 10 networks of length 12. Each network and therefore the pinwheel regions of each network have symmetry $\bar{3}m$ with the threefold axis parallel to the MCS edges to which the special points on the network belong. The networks are bipartite and therefore the pinwheel construction is possible.

The sizes of the pinwheel regions are limited by condition (P5). In this case, the pinwheel region about a given special point must not contain any points that are separated from any point in another pinwheel region by a constraint vector of length $2\sqrt{s\tau} \approx 1.7013$ which is along one of the icosahedral twofold direction that forms a 36° angle with the twofold direction of the constraint vector that links the special point with another special point on the same network. The effective constraint vectors for Eq. (13) are of length $\sqrt{s/\tau^3} \approx 0.3249$ along the 12 icosahedral twofold directions that form an angle of $\arccos(1/\sqrt{3}) \approx 54.7°$ with the axis of the pinwheel region. The pinwheel regions thus formed are shaped like the volume of intersection of two cubes of side length $\sqrt{s/\tau^3}$ that share a long diagonal and are rotated $\sqrt{3}/50\pi \approx 44.1°$ with respect to each other. This volume is shown in Fig. 12. When the pinwheel regions are half-filled, the new atomic surface volume is

$$V_\perp = 20 s^{3/2} \tau^{9/2} (1 - \tau^{-5} + \tau^{-9}/2 - \tau^{-12}/2) \tag{35}$$

and the packing fraction is $f \approx 0.5566$. Even with the pinwheel construction, the packing fraction remains well below the believed maximum.

Checking for iterations of the pinwheel construction, one finds no sets of new special points which do not produce odd-length loops in the supernetworks formed. In this case, the pinwheel construction cannot be iterated.

There exist certain interesting analogies between the icosahedral and octagonal sphere packing problems. In the octagonal sphere packing problem it has neither been proven nor disproven whether it is possible to cover the plane with octagonal symmetry using only the square and flattened hexagon as tiles. In the icosahedral case, it has neither been proven not disproven whether it is possible to cover space in a pattern with icosahedral symmetry using only the four canonical cells[25] as tiles. The MCS for each case introduce certain very poorly packed regions—there are octagons in the tiling projected from the octagonal MCS and there are icosahedra in the tiling formed by the nodes projected from the icosahedral MCS. The pinwheel construction is possible for each

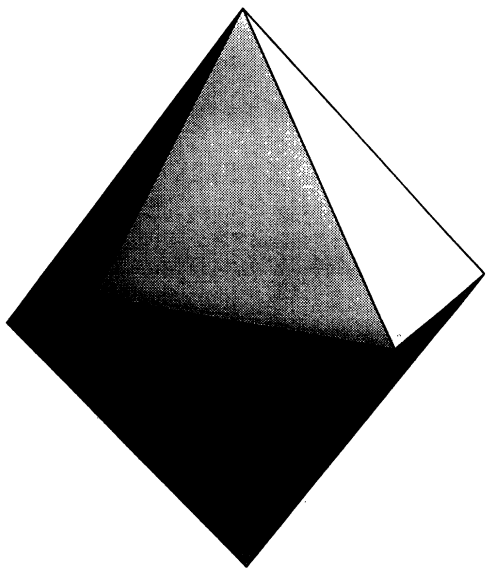

FIG. 12. Shape of pinwheel regions for the atomic surface shown in Fig. 11.

case, but does not get rid of all the poorly packed regions [see Fig. 7(f)]. Finally, the very poorly packed regions for each case are tiles whose center is not on a vertex of the higher-dimensional cubic lattice but rather on a body-center point. While the dodecagonal square-triangle tiling has been used as a 2D test case for the canonical cells model,[29] it seems that useful new insights into the icosahedral problem could be found by investigating the tilings corresponding to octagonal sphere packings as well.

V. THE PINWHEEL THEOREM IN PARALLEL SPACE

So far, this work has concentrated mainly on the pinwheel theorem's effect on the atomic surfaces in perp. space. In this section, the parallel space equivalent of the pinwheel theorem and pinwheel construction will be investigated, in particular, the nature of the regions that become better packed via the pinwheel construction.

In perp. space, the pinwheel theorem holds when there is a bipartite network consisting of N special points. The links in the network are constraint vectors. In parallel space, for points with $\mathbf{r}^{\perp}$ in the pinwheel regions, the projected structure contains a corresponding bipartite network where nodes are linked by vectors that are shorter than $d_{\min}$. In perp. space, the MCS is "convex" about the special points, that is, according to Eq. (9), $p(\mathbf{r}_s^{\perp})<\frac{1}{2}$, while, after the pinwheel construction $p(\mathbf{r}_s^{\perp})=\frac{1}{2}$. The parallel-space equivalent is that pN nodes on the projected network of the MCS are occupied, while $N/2$ of these nodes are occupied after the pinwheel construction. In the dodecagonal case, for example, $N=12$ and $p(\mathbf{r}_s^{\perp})=\frac{5}{12}$, so in parallel space, 5 out of 12 of the nodes in the projected network are occupied before the pinwheel construction and 6 out of 12 are occupied after the pinwheel construction. These nodes plus other nearby nodes that are necessary to build tiles form a region that will be termed a "repackable volume."

In addition, the pinwheel construction has an arbitrariness as to which subnetwork of each network of points in the pinwheel regions is occupied. There are always two different parallel-space packings of the repackable volume corresponding to whether the even or the odd nodes of the network are occupied. The repackable volumes, their "poorly packed" tilings before the pinwheel construction, and their two "well-packed" tilings for each structure to which the pinwheel construction has been applied will now be given. For all cases here, the exterior of the repackable volume has the point group of the network of special points, G_i, but the decoration of the interior lowers the symmetry to that of the subgroup of G_i consisting of the elements g_{ij} whose parity, as defined in Sec. II, satisfies $P(g_{ij})=0$.

In the dodecagonal case, the repackable volume corresponding to the first stage of the pinwheel construction consists of 12 triangles and 6 squares. The exterior of this region is a dodecagon. The poorly packed tiling and the two well-packed tilings of this volume are shown in Fig. 13. In essence, the pinwheel construction replaces two distorted hexagons with four triangles and three squares. The poorly packed tiling of the repackable volume for octagonal symmetry and the two well-packed tilings of this volume are shown in Fig. 14. The first stage of the pinwheel construction essentially destroys two concave octagons and replaces them with one square and three flattened hexagons. Numerous poorly packed tilings of repackable volumes can be seen in Figs. 2(d) and 7(d), corresponding to structure based on MCS's. In Figs. 2(e) and 7(e), representing the corresponding tilings after the pinwheel construction, many of the poorly packed tilings are seen to be replaced by well-packed tilings. Finally, the repackable volume of the icosahedral b-c network is shown in Fig. 15. The pinwheel construction makes this region well packed, consisting of 42 A cells, 18 B cells, 20 C cells, and 6 D cells. Including the interior, the point group of each well-packed tiling is $\bar{3}$. Before the pinwheel construction, the interior is poorly packed and contains noncanonical cells. This region was independently discovered by Oxborrow[30] in the study of canonical cell tilings and is believed to be the smallest rearrangeable volume consisting of canonical cells.

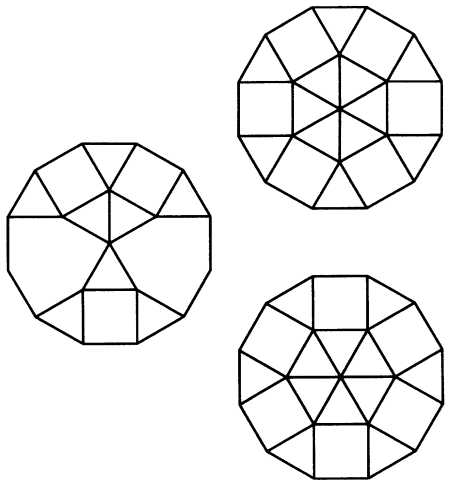

FIG. 13. Poorly packed and well-packed tilings of the repackable volume for the dodecagonal sphere packing problem.

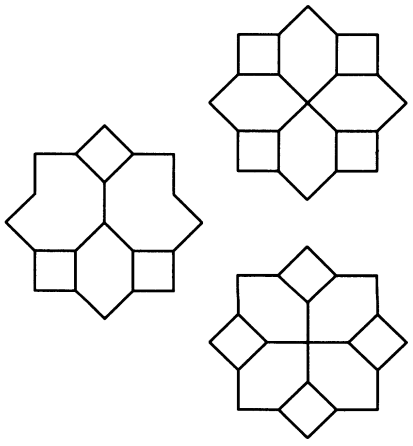

FIG. 14. Poorly packed and well-packed tilings of the repackable volume for the octagonal sphere packing problem.

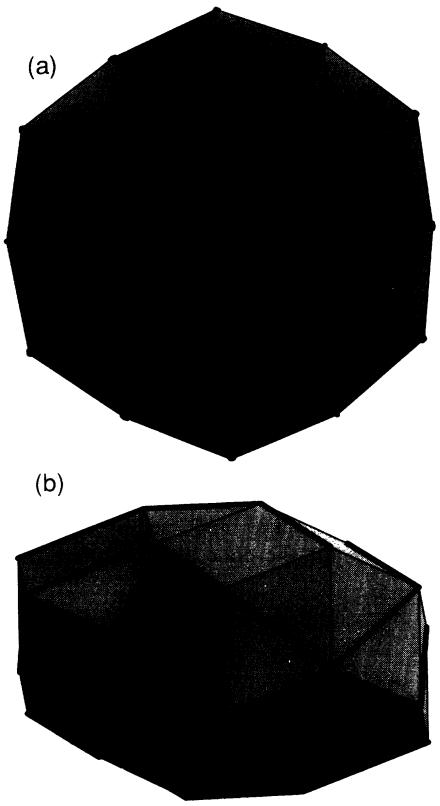

FIG. 15. (a) Top and (b) front views of the repackable volume for the $d_{\min} \approx 0.5628$ icosahedral sphere packing problem. Thick lines indicate linkages along icosahedral twofold directions (*b* linkages). The volume shown can be tiled with canonical cells in two different ways.

Amusingly, for the icosahedral case, $N=12$ and $p(\mathbf{r}_s^\perp)=\frac{5}{12}$, exactly as for the dodecagonal case, so the pinwheel construction again places six nodes on a network where only five nodes were occupied before.

Where the pinwheel construction is iterable, successive iterations repack regions of larger volume, as can be seen by comparing Figs. 2(e) and 7(e) with Figs. 2(f) and 7(f). It is to be noted that the shapes of the new repackable volumes become more complicated. The details of the shapes of these new repackable volumes have not yet been worked out.

VI. DERIVATION OF INFLATION RULES

Whenever the pinwheel construction is infinitely iterable, the final atomic surface is fractal. It is then difficult to compute the value of $f(\mathbf{r}^\perp)$ for $\mathbf{r}^\perp$ near the boundary of the fractal and thus it is difficult to calculate the parallel space structure corresponding to the fractal atomic surface.

A more practical way of generating quasiperiodic structures corresponding to such complicated atomic surfaces is by inflation, if an inflation rule exists. Historically, the inflation rule for the square-triangle tiling was found first,[15] then this rule was found to lead to fractal atomic surfaces.[18] Here, the problem is considered in reverse: given a fractal atomic surface produced by the iterated pinwheel construction, what, if any, inflation rule is implied?

Inflation is a general property of the quasicrystalline symmetries considered in this work,[8,21] that is, if the atomic surface is kept the same and the transformation $\mathbf{e}_i^\parallel \rightarrow \sigma \mathbf{e}_i^\parallel$ and $\mathbf{e}_i^\perp \rightarrow \pm \mathbf{e}_i^\perp/\sigma$ is performed, with σ such that the D-dimensional lattice is mapped onto itself, then the new structure is indistinguishable from the old one. An equivalent operation is to (Ia) expanded the atomic surfaces about each point by a factor σ and then (Ib) take $\mathbf{e}_i^\parallel \rightarrow \sigma \mathbf{e}_i^\parallel$. What we seek is an inflation rule in a stronger sense, where the expansion of the atomic surfaces replaces each node in parallel space with a set of nodes in a manner that is equivalent for all nodes.

Simple inflation rules are possible for special atomic surface shapes. Let A be the atomic surface and let σA be the expansion of A by a factor of σ. Now if the set of images of A, $\{A+\Delta\mathbf{r}_i^\perp\}$, with $\Delta\mathbf{r}_i^\perp=\sum \Delta n_{ij}\mathbf{e}_j^\perp$ completely covers σA without covering points not in σA, then $\mathbf{r}^\parallel \rightarrow \{\mathbf{r}^\parallel+\Delta\mathbf{r}_i^\parallel\}$, with $\Delta\mathbf{r}_i^\parallel=\sum \Delta n_{ij}\mathbf{e}_j^\parallel$, is a simple rule for step (Ia) of the inflation process for the structure.[31]

The inflated atomic surface of the iterated pinwheel construction for dodecagonal symmetry can be completely covered with translations of the original atomic surface if we include *all* of the pinwheel regions as part of the atomic surface for the time being. The general inflation symmetry for dodecagonal quasicrystals, $\mathbf{e}_0^\parallel \rightarrow 2\mathbf{e}_0^\parallel + 2\mathbf{e}_1^\parallel - \mathbf{e}_3^\parallel$, etc., has $\sigma=2+\sqrt{3}$. Since each step of the iterated pinwheel construction places dodecagons of linear scale $1/\sigma$ that of the preceding dodecagons about the corners of the preceding dodecagons, in the atomic surface expanded by σ, the pinwheel regions can be exactly congruent to the original complete atomic surface. Furthermore, the displacements of the centers of these 12 pinwheel regions from the center of the expanded atomic surface have integer coordinates $\{g_i(2\mathbf{e}_0^\perp-2\mathbf{e}_1^\perp+\mathbf{e}_3^\perp)\}$, as is necessary for inflation. However, the translations just found are insufficient to cover the expanded atomic surface. If the translations $(\mathbf{0})$ and $\{g_i(\mathbf{e}_0^\perp-\mathbf{e}_2^\perp-\mathbf{e}_3^\perp)\}$ are added to the above set, the set of translated surfaces then does cover σA completely.

The parallel-space equivalent to the inflation rule (Ia) just found is to replace each node with the set of nodes shown in Fig. 16. The new nearest-neighbor distance between nodes should be $1/(2+\sqrt{3})$ that of the old nearest-neighbor distance. One can see that adjacent vertices of the central dodecagon violate the minimum separation constraint. This is because the atomic surface that generates this structure is one in which the pinwheel regions are entirely filled, while in reality they are only half filled. Half-filled pinwheel regions mean that only six of the inner dodecagon points are occupied, thus in the true inflation rule, each node is replaced by a set of tiles containing a central hexagon in one of the two orientations shown in Fig. 13.

The only difficulty left is in determining the orientation of the interior hexagon for each inflation step. This can be done by applying a rule for filling the pinwheel to the pinwheel construction and then using this rule along with perp.-space information about each node to be inflated to

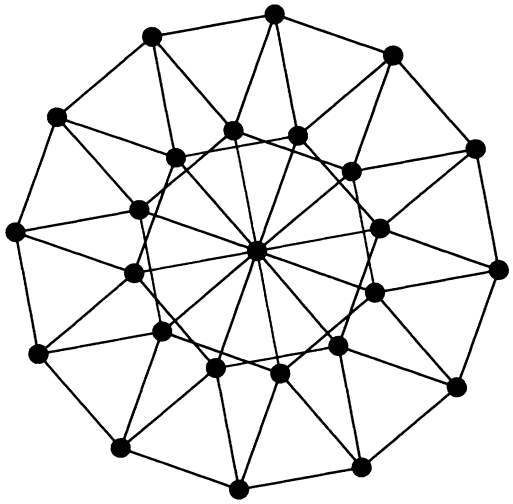

FIG. 16. Parallel-space inflation for the fractal atomic surface for the square-triangle tiling with the pinwheel regions completely filled. In the actual atomic surface, the pinwheel regions are only half filled, and thus in the actual inflation rule only one of the hexagonal sets of nodes in the interior is occupied, as in Fig. 13.

determine the orientation of the inner hexagon upon inflation. Alternately, a local inflation rule that maintains full dodecagonal symmetry and that never makes use of perp.-space information is to take a random choice of hexagon orientation at each inflation step.[15] In perp. space, the function $f(\mathbf{r}^{\perp})$ is taken to be randomly 0 or 1 for each value $\mathbf{r}^{\perp} \in S_i$. Note that the value of the function in various wedges of S_i are no longer related by symmetry; however, the average of $f(\mathbf{r}^{\perp})$ over any finite volume within S_i is exactly $\frac{1}{2}$ so perfect dodecagonal symmetry is maintained. This is the random Stampfli inflation rule.

In the octagonal case, the appropriate linear inflation factor σ is equal to $1+\sqrt{2}$. In contrast to the dodecagonal case, the pinwheel regions of σA are not congruent to A. No translations of A cover the pinwheel regions without overlap. Therefore, no simple inflation rule exists for this structure. It seems plausible that there could be some more complicated inflation rule for this structure because each step of the iterated pinwheel construction after the first step places octagons whose sides are $1/\sigma$ that of the preceding octagons about the corners of the preceding octagons, so there is some self-similarity under expansion of the atomic surface. However, no specific inflation rule has yet been determined.

The icosahedral b-c packing described, while arising from a pinwheel construction, does not arise from an atomic surface with self-similarity, therefore there is no inflation rule for generating it. This does not mean that there is no inflation rule for any b-c packing.

VII. LIMITATIONS OF THE PINWHEEL THEOREM

The pinwheel construction has proven useful in the octagonal, dodecagonal, and icosahedral sphere packing problems. However, the pinwheel construction is not powerful enough to always produce the highest-density packings. This section mentions some other ways in which the density of a quasicrystalline sphere packing can be increased over that produced by cutting a lattice of MCS. Only the one-component sphere packing problem is considered throughout.

A. Relaxation of nodes from "ideal" positions

This work has maintained the assumption that the atomic surfaces have no component along physical space, that is, the atomic positions upon projection are always $\mathbf{r}_c^{\parallel}$, where $\mathbf{r}_c$ is the position of the center of the atomic surface. More generally, it is possible to have displacements of the atoms, that is, to have the atomic surface centered at $\mathbf{r}_c$ to contain points whose parallel component is $\mathbf{r}_c^{\parallel}+\delta\mathbf{r}^{\parallel}$. The atoms in a real solid obey physical interactions and know nothing about perp. space. One would thus suspect that in any real material, atoms placed at "ideal" positions would relax away from these positions. Conceivably, the poorly packed regions of the structures found would be compressed, leading to a larger $d_{\min}$ in the relaxed structure than for the model and thus a higher packing fraction.

B. Use of "nonmonatomic" lattices

It is often possible to find structures that have a higher packing fraction than those projected from a D-dimensional Bravais lattice of a single atomic surface shape. One way of increasing the packing fraction is to place more than one atomic surface shape on the lattice points. By using one atomic surface at the even nodes of the 6D cubic lattice and a different atomic surface at the odd nodes, Audier and Guyot[6,32] were able to achieve a packing fraction of 0.5583 (Ref. 25) for an icosahedral b-c network. This structure has face-centered icosahedral symmetry, the symmetry observed in the AlCuFe family of quasicrystals.

A second way of increasing the packing fraction is by adding additional atomic surfaces centered at other points in the higher-dimensional lattice. In the octagonal case, one could add a node to the center of each octagon in the tiling. This is equivalent to adding an atomic surface shaped like a small octagon to each body center of the 4D cubic lattice and increases the packing fraction to approximately 0.6723. In the icosahedral case, it is possible to include atomic surfaces to half of the body-center positions of a face-centered icosahedral structure to obtain a packing fraction of

$$f=\frac{\pi}{2}\left[\frac{3}{4}\right]^{1/2} s(1-\tau^{-5}+\tau^{-6}/2)\approx 0.5705\ . \qquad (36)$$

The network now contains linkages of length τ^{-1} in icosahedral fivefold directions and is an example of an icosahedral a-b-c network. Surfaces that yield this packing fraction were found independently by Cockayne *et al.*[2] and by Katz and Gratias.[3] In addition to the higher packing fraction, the structure is a model for the actual atomic positions in the AlCuFe family of icosahedral quasicrystals.

C. Use of alternative higher-dimensional lattices

The higher-dimensional lattice used here for decagonal symmetry with $D=4$ is nonstandard. The higher-dimensional lattice more commonly used is the $D=5$ cubic lattice used for the 2D Penrose tiling. Such a lattice has an associated $D-d=$three-dimensional perp. space. One packing based on this lattice[24] has a packing fraction $f\approx 0.7386$, which exceeds any decagonal packing fraction found here.

D. Overpacking plus elimination

One commonly used method for generating quasiperiodic packings is to produce a structure, for example, by giving Penrose tiles a simple decoration, that has pairs of atoms that are too close, and then eliminating some points so as to eliminate these close pairs. This procedure was used to produce the Audier-Guyot icosahedral b-c packing and the decagonal packing described above. Henley eliminated points in the 3D Penrose tiling to produce an icosahedral a-b packing with a packing fraction $f\approx 0.6288$, even higher than that corresponding to the truncated stellated dodecahedron atomic surface.[24]

More recently, Mihalkovič and Mrafko have investigated icosahedral b-c networks by generating the nodes in a large-unit-cell periodic approximant corresponding to an oversized atomic surface and then using Monte Carlo methods to occupy a subset of these nodes to produce structures consisting entirely of canonical cells.[28,33] This work suggest that the atomic surface shapes corresponding to an icosahedral canonical cell tiling would be complicated and contain nonconnected regions.[28]

E. Random growth

Random growth of icosahedral b-c networks has been studied by Elser[26] and by Robertson and Moss.[27] They obtained the previously stated result that a packing fraction of 0.60 to 0.61 seems possible. The perp.-space map of the coordinates of the nodes in the Robertson-Moss packing suggest an atomic surface that, at the level of resolution corresponding to the finite size of their model, is a featureless "cloud" that is denser toward the center of the atomic surface.

F. Nonpinwheel rearrangements

One nonpinwheel method of increasing the packing fraction of a quasicrystalline sphere packing is of particular interest because it also produces nonconnected atomic surfaces. One looks at a projected structure for poorly packed regions other than the poorly packed regions found by the pinwheel construction. Then, these regions are repacked in a denser manner, and the repacking is translated into the perp.-space alteration of the atomic surface shape.

The method can be used in the decagonal sphere packing problem, where, as shown in Fig. 17, various regions obtained in projecting the MCS can be replaced by regions that are better packed. When this is done for every

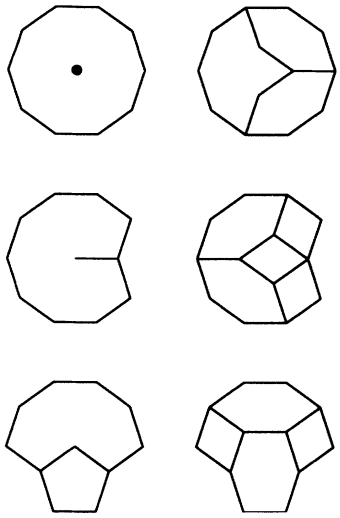

FIG. 17. Repackable volumes of the decagonal tiling shown in Fig. 9(c). These regions do not arise from the pinwheel theorem.

such region, the new atomic surface obtained is shown in Fig. 9(b). (Note that full decagonal symmetry is preserved.) This new atomic surface is not unique because there is some freedom in how to choose the orientations of the interiors of the decagons shown in Fig. 17. The new decagonal packing fraction is $f=(1+2\tau^{-5})f(\mathrm{MCS})\approx 0.7053$.

This construction is somewhat analogous to the pinwheel construction. The total volume is increased by replacing the connected atomic surface with one that has nonconnected pieces within regions centered on a set of points that form a network. Again there is some arbitrariness in how to choose $f(\mathbf{r}^{\perp})$ within these regions. Effective constraint vectors limit the size of the regions in which this construction can be done.

This construction differs from the pinwheel construction in that the network of "special points" may contain odd-length loops (as it does here) and need not be located on the original boundary of the MCS. Additionally, less than half of the regions involved in the construction are filled. Furthermore, the network of "special points" is not a single orbit of G.

It is possible to expand the volume of the icosahedral b-c network using a similar kind of construction. In parallel space, there are points that have seven neighbors in icosahedral threefold directions where it is possible to replace these neighbors with eight neighbors in a set of threefold directions that are congruent with the directions of a point to its nearest neighbors in a 3D bcc structure. In perp. space, this corresponds to expanding the MCS about its threefold vertices. Although the network that these vertices form has odd-length loops, the average volume filled around each point can be increased from $\frac{7}{20}$ to $\frac{8}{20}$. The volumes that can be so refilled are limited by additional constraint vectors. According to Eq. (13), the maximal volume about each special point that can be $\frac{8}{20}$ filled is a regular dodecahedron of fivefold radius 0.5.

The packing fraction achieved is

$$f=\frac{\pi}{2}\left[\frac{3}{4}\right]^{1/2} s(1-\tau^{-5}+5\tau^{-8}/8)\approx 0.5616\ . \quad (37)$$

These examples suggest the possibility that there is some generalization of the pinwheel theorem and pinwheel construction that could yield all possible ways of increasing the packing fraction of a quasicrystalline sphere packing. However, in contrast with the pinwheel construction, where the set of special points can be systematically determined, no systematic way of finding these other sets of "special points" has been found.

G. Combinations of methods

It is sometimes possible to use more than one method to improve the packing fraction for the quasiperiodic sphere packing problem. In particular, the pinwheel method, in combination with other local rearrangements, can be used on the icosahedral b-c packing. However, one must take care that the regions that are refilled via the pinwheel theorem do not overlap the regions refilled by the $\frac{7}{20}$ to $\frac{8}{20}$ improvement. A packing fraction of

$$f=\frac{\pi}{2}\left[\frac{3}{4}\right]^{1/2} s(1-\tau^{-5}+5\tau^{-8}/8+\tau^{-9}/2 -\tau^{-12}/2-\tau^{-14}/4)\approx 0.5645 \quad (38)$$

can be achieved by this process.

The $\frac{7}{20}$ to $\frac{8}{20}$ improvement is also possible for the icosahedral a-b-c packing described in this section, and improves the packing fraction to

$$f=\frac{\pi}{2}\left[\frac{3}{4}\right]^{1/2} s(1-\tau^{-5}+\tau^{-6}/2+5\tau^{-8}/8) \approx 0.5786\ . \quad (39)$$

This modification of the icosahedral a-b-c packing is proposed as a new model for the positions of the atoms in the AlCuFe family of icosahedral quasicrystals.

VIII. CONCLUSIONS

In this work, the quasiperiodic sphere packing problem has been investigated. The atomic surfaces for the most dense packings may be nonconnected. In fact, a simple test, the pinwheel theorem, can show that a given connected atomic surface is not the surface that leads to the densest packing.

The details of finding a nonconnected atomic surface of higher volume than the given connected surface are given. For the dodecagonal case, the atomic surface for the square-triangle tiling, a fractal, is the surface found by this procedure. It is found without incorporating any knowledge into the derivation that the final projected structure should consist of only squares and triangles.

However, although the pinwheel construction improves the packing fraction for an icosahedral b-c network over that obtained from a connected atomic surface, it does not produce the icosahedral b-c network of highest density. The existence of nonconnected atomic surfaces in the decagonal and icosahedral cases which do not arise from the pinwheel theorem leaves open the possibility that the pinwheel theorem is a special case of a more general technique that can be used in determining the highest-density quasicrystalline sphere packings.

ACKNOWLEDGMENTS

This work was funded by the U.S. Department of Education and by the David and Lucille Packard Foundation FDN89-1606. The author thanks V. Elser, C. L. Henley, M. Mihalkovič, M. E. J. Newman, M. Oxborrow, and A. P. Smith for useful discussions and thanks V. Elser and C. L. Henley for their comments on the manuscript.

*Present address: Laboratoire de Physique des Solides, Université Paris-Sud, Bâtiment 510, 91405 Orsay Cedex, France.

[1]M. Cornier-Quiquandon, A. Quivy, S. Lefebvre, E. Elkaim, G. Heger, A. Katz, and D. Gratias, Phys. Rev. B **44**, 2071 (1991).

[2]E. Cockayne, R. Phillips, X. B. Kan, S. C. Moss, J. L. Robertson, T. Ishimasa, and M. Mori, J. Non-Cryst. Solids **153&154**, 140 (1993).

[3]A. Katz and D. Gratias, J. Non-Cryst. Solids **153&154**, 187 (1993).

[4]P. Guyot and M. Audier, Philos. Mag. B **52**, L15 (1985).

[5]V. Elser and C. L. Henley, Phys. Rev. Lett. **55**, 2883 (1985).

[6]M. Audier and P. Guyot, Philos. Mag. B **53**, L43 (1986).

[7]A. P. Smith, Phys. Rev. B **42**, 1189 (1990).

[8]N. de Bruijn, Ned. Akad. Weten. Proc. Ser. A **84**, 39 (1981); **84**, 53 (1981).

[9]P. Kramer and R. Neri, Acta Crystallogr. A **40**, 580 (1984).

[10]P. A. Kalugin, A. Yu. Kitaev, and L. S. Levitov, Piz'ma Zh. Eksp. Teor. Fiz. [JETP Lett. **41**, 47 (1985)].

[11]V. Elser, Phys. Rev. B **32**, 4892 (1985).

[12]M. Duneau and A. Katz, Phys. Rev. Lett. **54**, 2688 (1985).

[13]P. Bak, Scr. Metal. **20**, 1199 (1986); Phys. Rev. Lett. **56**, 861 (1986).

[14]C. L. Henley, in *Quasicrystals: The State of the Art,* edited by D. P. DiVincenzo and P. J. Steinhardt (World Scientific, River Edge, New Jersey, 1991).

[15]P. Stampfli, Helv. Phys. Acta **59**, 1260 (1986).

[16]P. W. Leung, C. L. Henley, and G. V. Chester, Phys. Rev. B **39**, 446 (1989).

[17]A. P. Smith, J. Non-Cryst. Solids **153&154**, 258 (1993).

[18]M. Baake, R. Klitzing, and M. Schlottmann, Physica A **191**, 554 (1992).

[19]Fractal atomic surfaces for related dodecagonal quasicrystals were noted by F. Gähler, Doctoral dissertation, Swiss Federal Institute of Technology, Zürich, 1988.

[20]C. Godrèche, J. M. Luck, A. Janner, and T. Janssen, J. Phys. I (France) **3**, 1921 (1993) studied the related octagonal square-rhombus tiling and found fractal and nonconnected atomic surfaces for certain tilings.

[21]J. E. S. Socolar, Phys. Rev. B **39**, 10 519 (1989).

[22]D. Shechtman, I. Blech, D. Gratias, and J. W. Cahn, Phys. Rev. Lett. **53**, 1951 (1984).

[23]C. Oguey and M. Duneau, Europhys. Lett. **7**, 49 (1988).

[24]C. L. Henley, Phys. Rev. B **34**, 797 (1986).

[25]C. L. Henley, Phys. Rev. B **43**, 993 (1991).

[26]V. Elser, in *Aperiodicity and Order 3: Extended Icosahedral Structures,* edited by M. Jaríc (Academic, New York, 1989).

[27]J. L. Robertson and S. C. Moss, Z. Phys. B **83**, 391 (1991).
[28]M. Mihalkovič and P. Mrafko, Europhys. Lett. **21**, 463 (1993).
[29]M. Oxborrow and C. L. Henley, J. Non-Cryst. Solids **153&154**, 210 (1993); Phys. Rev. B **48**, 6966 (1993).
[30]M. Oxborrow (private communications).
[31]Conversely, a simple inflation rule leads to a self-similar atomic surface that is often a fractal, as shown by J. M. Luck, C. Godrèche, A. Janner, and T. Janssen, J. Phys. A **26**, 1951 (1993).
[32]P. Guyot, M. Audier, and R. Lequette, J. Phys. (Paris) Colloq. **47**, C3-389 (1986).
[33]M. Mihalkovič and P. Mrafko, J. Non-Cryst. Solids **143**, 225 (1992).

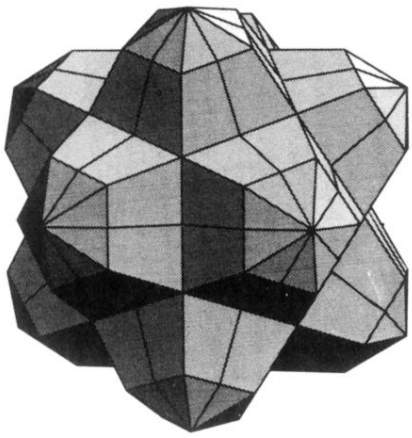

FIG. 10. Truncated stellated dodecahedron atomic surface for the $d_{\min} = 1$ icosahedral sphere packing problem.

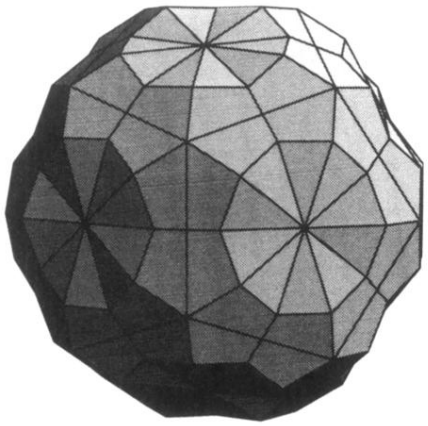

FIG. 11. Truncated triacontahedron atomic surface for the $d_{\min} \approx 0.5628$ icosahedral sphere packing problem.

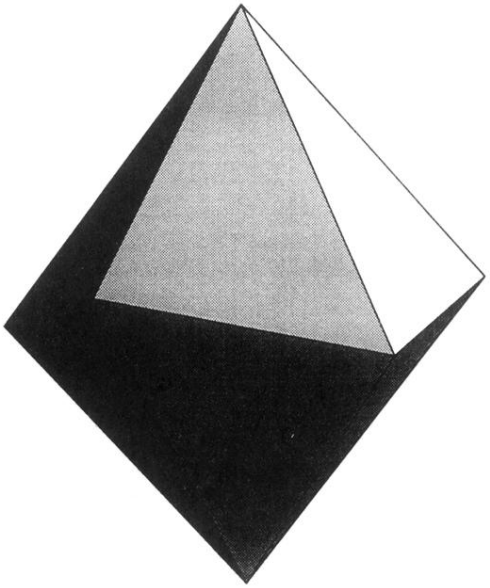

FIG. 12. Shape of pinwheel regions for the atomic surface shown in Fig. 11.

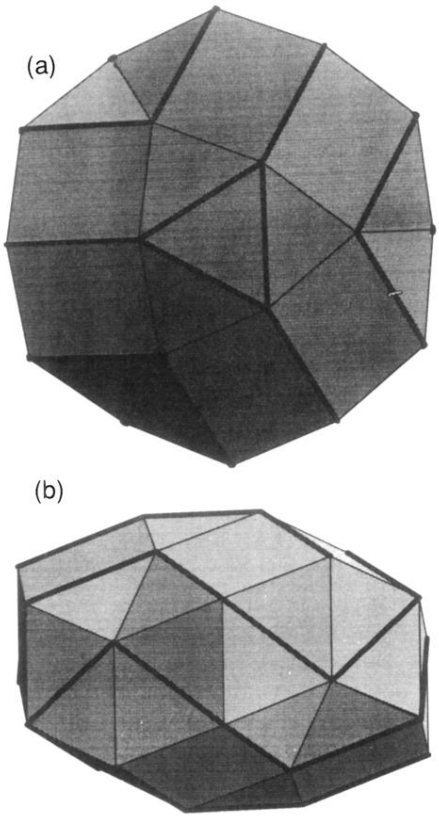

FIG. 15. (a) Top and (b) front views of the repackable volume for the $d_{\min} \approx 0.5628$ icosahedral sphere packing problem. Thick lines indicate linkages along icosahedral twofold directions (b linkages). The volume shown can be tiled with canonical cells in two different ways.

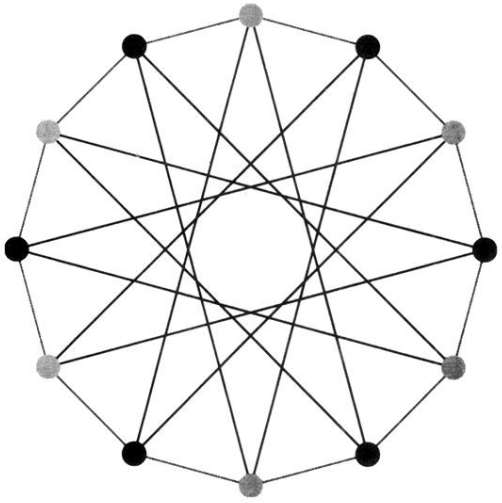

FIG. 3. Special points of the dodecagonal MCS and the network that they form. The special points are indicated by circles. The interior lines are the constraint vectors that form the links of the network. The two colorings of the special points indicate how the network is bipartite.

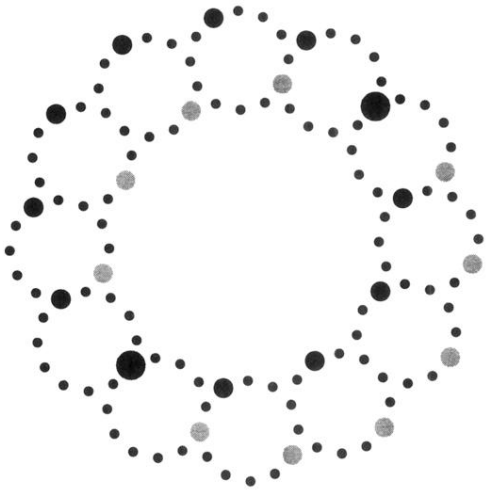

FIG. 6. New special points for the second stage of the iterated pinwheel construction for dodecagonal symmetry. The medium gray circles indicate new special points on one network like that in Fig. 3; the large solid circles indicate special points on another network. The two networks share the points indicated by the largest solid circles and thus are linked in the supernetwork of such networks.